Optics Letters

Phase noise characterization of sub-hertz linewidth lasers via digital cross correlation

Xiaopeng Xie,[1] Romain Bouchand,[1] Daniele Nicolodi,[1,2] Michel Lours,[1] Christophe Alexandre,[3] and Yann Le Coq[1,*]

[1]LNE-SYRTE, Observatoire de Paris, PSL Research University, CNRS, Sorbonne Universités, UPMC Univ. Paris 06, 61 avenue de l'Observatoire, 75014 Paris, France
[2]Currently at National Institute of Standards and Technology (NIST), 325 Broadway, Boulder, Colorado 80305, USA
[3]CNAM, CEDRIC Laboratory, 292 rue Saint Martin, 75003 Paris, France
*Corresponding author: yann.lecoq@obspm.fr

Received 20 December 2016; revised 18 February 2017; accepted 19 February 2017; posted 24 February 2017 (Doc. ID 283242); published 17 March 2017

Phase noise or frequency noise is a key metric to evaluate the short-term stability of a laser. This property is of great interest for the applications but delicate to characterize, especially for narrow linewidth lasers. In this Letter, we demonstrate a digital cross-correlation scheme to characterize the absolute phase noise of sub-hertz linewidth lasers. Three 1542 nm ultra-stable lasers are used in this approach. For each measurement, two lasers act as references to characterize a third one. Phase noise power spectral density from 0.5 Hz to 0.8 MHz Fourier frequencies can be derived for each laser by a mere change in the configuration of the lasers. To the best of our knowledge, this is the first time showing the phase noise of sub-hertz linewidth lasers with no reference limitation. We also present an analysis of the laser phase noise performance.

OCIS codes: (120.0120) Instrumentation, measurement, and metrology; (120.5050) Phase measurement; (140.0140) Lasers and laser optics.

https://doi.org/10.1364/OL.42.001217

Laser phase noise describes how the phase of a laser output electrical field deviates from an ideal sinusoidal wave. This quantity, which is defined to evaluate the short-term stability of a laser, can also be used to estimate the linewidth or coherent length of a laser. In many applications, such as coherent optical communication [1], LIDAR [2], optical fiber-based interferometric sensors [3], high resolution spectroscopy [4], ultra-low phase noise photonic microwave generation [5], and optical atomic clock [6], the laser phase noise can profoundly impact the limitation of a system. Thus, lasers with ultra-low phase noise are actively studied [7–10], while the precise characterization of such ultra-stable lasers is becoming more important.

Phase noise characterization is a comparison process. Generally, laser phase noise measurement approaches can be divided into two categories according to the comparison method. The first one is comparing the laser under test with itself through the schemes of delayed self-homodyne, delayed self-heterodyne [11,12], or Michelson interferometer [13]. Several kilometers of fiber are usually used for these optical delay line methods in order to make the delay time longer than the laser coherent time. It is difficult to characterize the phase noise of lasers with hundreds-hertz linewidth or narrower via these delay line technique as thousands of kilometers of fiber would be required, and the fiber noise itself can also become a limitation. The second category, which is called the beat-note method [14–17], implies comparing the laser under test with a reference laser whose phase noise is much lower than that of the one under test. When the phase noise of the laser under test is lower than that of any available reference, two similar lasers must be built and compared. Assuming statistical independence and equal contribution of both lasers, the phase noise is revealed after division of the beat-note phase noise by $\sqrt{2}$. However, to realize two equally good lasers is not straightforward.

Cross correlation is a well-known approach to characterize the phase noise of RF and microwave oscillators with ultra-low levels [5,18–22]. Here, we extend this approach to precisely characterize the phase noise of sub-hertz linewidth lasers. Three ultra-stable 1542 nm lasers are introduced in our system. Two of them act as references and beat with the one under test to generate two radio frequency electrical signals after photodetection. These two beat notes are analyzed by a home-designed digital heterodyne cross correlator [5,21]. Both of the electrical beat-note signals carry the phase information of the laser under test. As noise contributions from the two other optical sources are statistically independent, the phase noise power spectral density (PSD) of the laser under test is revealed by averaging the statistical estimator of the cross PSD of the phases of these two beat-note signals. Unlike the traditional beat-note phase noise characterization, the reference lasers in this cross-correlation system do not need to possess better phase noise level than that of the laser under test. Note that this is, in a sense, similar to the so-called three-cornered hat method [23]. However, our system provides the full phase noise PSD of the laser under test. Furthermore in this work, we switch

the role of the three lasers so as to characterize the absolute phase noise of each of them. Phase noise PSDs from 0.5 Hz to 0.8 MHz Fourier frequencies are shown for these three lasers. Additionally, the phase noise performance is analyzed.

Figure 1 shows our cross-correlation scheme to characterize the phase noise of narrow linewidth lasers. These three lasers achieve narrow linewidth regime through active stabilization of the semiconductor laser diode to the ultra-stable cavity by the Pound–Drever–Hall (PDH) method [24]. As these three lasers are located in two different rooms, their output lights are transmitted through tens of meters of fiber to the optical table where the photodiode is settled. The fiber links are noise-cancelled by the acousto-optic modulator-based feedback [25]. Fiber polarization controllers are used on each reference laser branch to reach sufficient beat-note signal power. The frequency differences between each pair of lasers are within 600 MHz.

To precisely characterize the phase noise of Laser B (under test), it is beat with two distinct reference lasers (A and C), as is presented in Fig. 1. These beat notes are separately detected by fast InGaAs photodiodes in channels X and Y. The output power of the photodiode is below −40 dBm. An RF amplifier with 20 dB gain is used after the photodiode. The first stage of our home-designed digital cross correlator is analog to digital conversion (ADC) at 250 mega sample per second (MSPS), which requires input frequencies below 125 MHz to obey Nyquist criterion. A frequency synthesizer, therefore, acts as the local oscillator to down-convert the carrier frequency of the beat-note signal to approximately 10 MHz (the two channels X and Y do not need to have exactly the same frequency). The down-converted signals are power-amplified, low-pass filtered, sent into two different ADCs, and fed to a field-programmable-gate-array (FPGA) based digital cross correlator. The internal structure of this digital correlator is similar with we reported in [5,21]. The digitized samples are demodulated in digital down conversion logic units, providing two phase data streams at 2 MSPS, which are then transferred by a gigabit Ethernet link to a computer for easy data analysis. Data streams are frequency de-drifted before they are analyzed, which is to overcome the frequency drift of laser cavity during the measurement. As both of these phase data sets from Channel X and Channel Y carry the phase information of the laser under test, averaging the cross phase noise PSD S_{YX} of these two data sets converges toward the phase noise PSD S_{BB} of the laser under test [18]:

$$\begin{aligned}\langle S_{YX}\rangle_m &= \frac{2}{T}\langle YX^*\rangle_m = \frac{2}{T}\langle [B+C]\times[B+A]^*\rangle_m \\ &= \frac{2}{T}[\langle BB^*\rangle_m + \langle BA^*\rangle_m + \langle CB^*\rangle_m + \langle CA^*\rangle_m] \\ &= S_{BB} + O\left(\sqrt{1/m}\right), \end{aligned} \tag{1}$$

where m is the average number, T is the measurement time. As three lasers are statistically independent, the cross terms decrease with a speed of 5 log[m] dB during the averaging process until it reaches the final phase noise PSD of the laser under test. Note that reference lasers with levels of phase noise higher than that of the laser under test are possible but require a longer measurement time. For instance, if the reference lasers exhibit phase noise levels one order of magnitude higher than that of the laser under test, our system requires a longer time to converge to the final phase noise PSD of the laser under test (for example, it can take up to 1 h for the first decade). In fact, these two time-dependent data sets from channels X and Y do not only take the noise from the reference laser, but also carry the noise of photodiode, local oscillator synthesizers, and the digital cross correlator. The noise added by the photodiode, the local oscillator synthesizers, and the digital cross correlator are far below the phase noise of the lasers we characterize. Furthermore, and more importantly, they are also for a large part statistically independent, and thus are averaged out during the laser phase noise characterization.

Figure 2 presents the electrical spectra of the beat-note signals measured before the mixer. The carrier frequencies of these two beat notes after the photodiode are 555 and 303 MHz, respectively. From the electrical spectra of the beat note, we can infer that the linewidths (full width at half-maximum [FWHM]) of all these lasers are narrower than 1 Hz, but this estimation is limited by the resolution bandwidth of the electrical spectrum analyzer. In Fig. 2(a), the symmetrical bump around 250 kHz offset frequency is due to one of the PDH locks (from laser under test or reference laser A). The same situation is observed in Fig. 2(b), but the locking bump is around 20 kHz. Combining the information from Figs. 2(a) and 2(b), the locking bump can be deduced to originate from the reference lasers, but not the laser under test, as the locking bump offset frequencies are different in these two figures. Averaging the cross phase noise PSD of these beat-note signals can give the individual laser under test information.

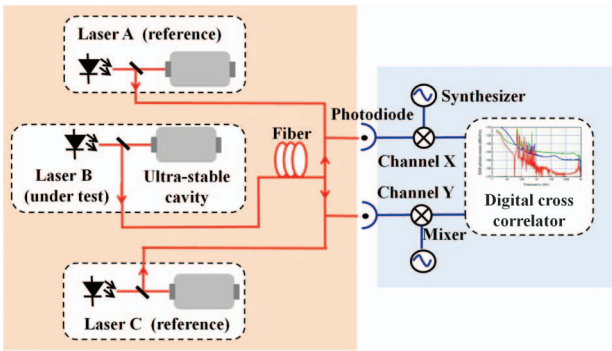

Fig. 1. Experimental setup of the laser phase noise characterization. Three separate ultra-stable 1542 nm lasers are used in this scheme. Laser B is beat with the reference Laser A and Laser C to get two electrical signals. These two electrical signals are first mixed down to a lower frequency and then analyzed by a home-designed digital cross correlator to reveal the phase noise PSD of Laser B.

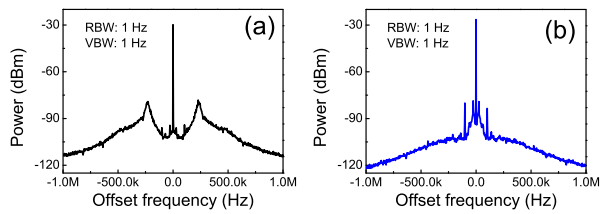

Fig. 2. Electrical spectra of the laser beat-note signals. RBW, resolution bandwidth; VBW, video bandwidth. (a) Beat note between Laser B (under test) and reference Laser A. (b) Beat note between Laser B and reference Laser C.

Figure 3 displays the typical result obtained for characterizing Laser B by the cross-correlator device. All phase noise PSD plots span to 0.8 MHz as the effect of the low-pass filter. Black and blue curves correspond to direct PSD of phase comparison between Laser B and Laser A (black) and Laser C (blue). These curves are in very good agreement with the corresponding electrical spectra shown in Fig. 2. In particular, the PDH phase locking bumps at 250 kHz (black) and 20 kHz (blue) clearly correspond to the similar features seen on the spectra displayed on Fig. 2. The red curve corresponds to the cross phase PSD result, and therefore to the absolute phase noise PSD of Laser B, assuming statistical independence between the phase fluctuations of A, B, and C. In this curve, it appears obvious that the previously observed servo bumps are coming from lasers A and C, while the servo bump of Laser B is much lower, and dwarfed in the A–B beat-note comparison by that of Laser A. In the blue curve, on the contrary, the minor feature near 250 kHz is indeed coming from the servo bump of Laser A, whereas the largest bump near 20 kHz is a feature of Laser C alone.

Furthermore, we can also observe that at low Fourier frequencies from 0.5 to 10 Hz, the phase noise of Laser B is higher than that of the reference Laser A, thus limiting the phase noise PSD of the beat note between lasers B and A. These slight differences between three lasers at different Fourier frequencies can be precisely characterized by the cross-correlator system, which is one of the attractive features of this laser phase noise measurement method.

By switching the respective roles of the lasers in Fig. 1, we can also iteratively characterize the phase noise of the other two lasers A and C. Figure 4 presents the final phase noise PSD results of all three lasers obtained this way. For all these lasers, the phase noise from 1 kHz to 1 MHz Fourier frequencies is limited by the PDH locking finite gain and bandwidth combined with the free running noise of the semiconductor lasers used in the servo loop. From looking at the locking bumps, it is obvious that the three lasers have different PDH locking bandwidths. This phase-locking bandwidth could be improved by using lower noise lasers and optimizing the loop filter circuit and feedback capability. Below 1 kHz Fourier frequencies, one observes some spurs that do not average down, even after several hours. They are partly caused by the 50 Hz and its harmonics from the various DC power supplies in the experiment, and partly by the acoustic noise of the fiber links that transmit the laser signals to the photodiodes. As shown in Fig. 5, the fiber link noise can reject up to 10 dB of acoustically-induced phase noise for certain Fourier frequencies. The ultra-stable cavity systems are carefully enclosed in acoustically isolating boxes. However, even when the fibers connecting the various systems together are noise cancelled, there remains approximately 2 m of fiber that could not be noise cancelled right before the laser beat-note generation. We believe these un-noise compensated fibers to be the main remaining sources of acoustic noise in the system. Note that sometimes spurs on the two channels have negative correlation during the measurement, like the tiny spur at 25 kHz in Fig. 4. The phase noise PSD at low Fourier frequencies is determined by the fractional frequency stability of the ultra-stable cavity to which the laser is locked. In our case, electrical noise contributions in the PDH locking make these phase noise curves depart from the thermal noise limit of the ultra-stable cavity [26]. The phase noise PSD values of these three lasers at 1 Hz offset are comparable but slightly different. According to the relationship between the phase noise and frequency noise,

$$S_v(f) = f^2 S_\varphi(f), \tag{2}$$

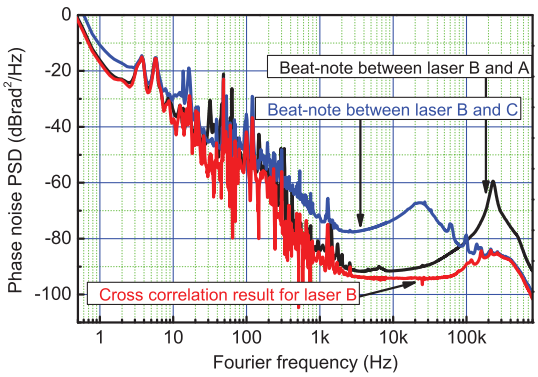

Fig. 3. Blue and black: phase noise PSDs for the beat notes of Laser B (under test) and the two references lasers (A and C). Phase noise PSD of the beat note includes the contribution from both the laser under test and the corresponding reference laser. Red: cross phase PSD result. This represents the absolute phase noise PSD of the laser under test, which is obtained by the heterodyne cross correlator.

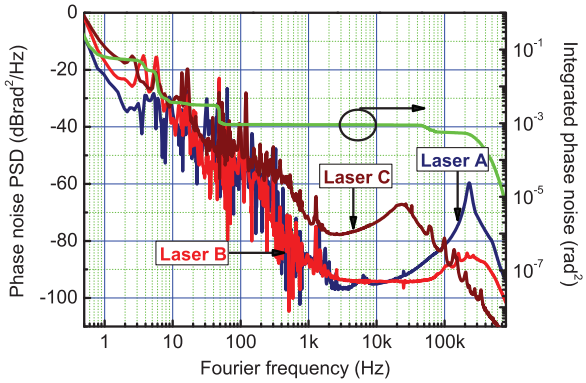

Fig. 4. Individual absolute phase noise PSDs of all three lasers used in the cross-correlation scheme. The phase noise PSDs of the two reference lasers A and C are characterized just by switching their roles in the cross-correlation scheme. The green curve is the integrated phase noise of Laser B.

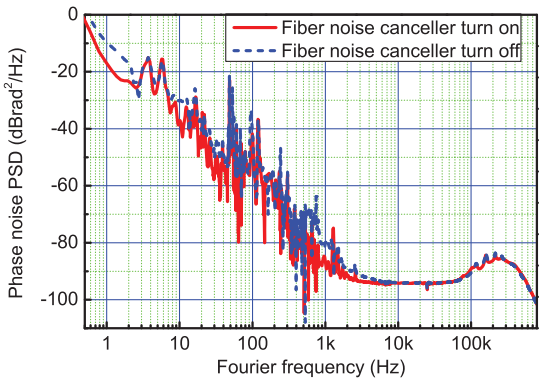

Fig. 5. Phase noise PSD of the narrow linewidth laser is affected by the acoustic noise at low Fourier frequencies.

where $S_\varphi(f)$ is the phase noise PSD, $S_v(f)$ is the frequency noise PSD, and f is the Fourier frequency, we can convert the phase noise PSD in Fig. 4 to frequency noise PSD very easily. Meanwhile, one possible relation between FWHM linewidth and phase noise can be defined as follows [27]:

$$\int_{\frac{\delta v}{2}}^{+\infty} S_\varphi(f)\mathrm{d}f = \frac{2}{\pi}, \tag{3}$$

where δv is the FWHM linewidth of the laser. From the phase noise measurement result, we can verify that, with this definition, all three lasers have linewidths narrower than 1 Hz. This fact is exemplified in Fig. 4, where the integrated phase noise from high Fourier frequencies down to lower Fourier frequencies is plotted and is shown to remain substantially below $2/\pi$ until 0.5 Hz Fourier frequency and lower.

In summary, we have successfully characterized the phase noise of sub-hertz linewidth lasers by using a FPGA-based heterodyne cross correlator. The noise floor of the homemade cross correlator is far below the phase noise of any reported ultra-narrow linewidth laser [5]. In order to characterize the phase noise of an individual narrow linewidth laser by cross-correlation, we have to use two additional reference lasers. The frequency difference between the laser under test and reference lasers needs here to remain within the bandwidth of the photodiode that converts the optical beat notes to electrical signals. Using an extra optical frequency comb could overcome this frequency bandwidth limitation. In a few words, provided the laser under test and the optical frequency comb provide a large enough optical beat-signal-to-noise ratio, phase locking one of the optical frequency comb lines to the laser under test could transfer the spectral properties of the laser under test to each comb line, and thus offer a bandwidth equal to that of the optical frequency comb, i.e., hundreds of nanometers [28]. In this way, beating the reference lasers with the comb lines nearest to their carrier optical frequencies would produce electrical beat notes that carry information about the phase of the laser under test. Averaging the cross phase PSD of the two beat notes generated by different reference lasers, with an extra added mathematical step to normalize the various measured phases to the carrier frequency of the laser under test, would produce the phase noise PSD of this laser. The demonstrated cross correlation method and its further developments will therefore be a useful tool to characterize the individual phase noise of extremely narrow linewidth lasers, regardless of their carrier optical frequencies.

Funding. Defense Advanced Research Projects Agency (DARPA) (W31P4Q-14-C-0050); Formation, Innovation, Recherche, Services et Transfert en Temps-Fréquence; Labex and Eurostar Eureka Program (Stable Microwave Generation and Dissemination over Optical Fiber project).

Acknowledgment. We thank José Pinto for help with the electronics and Rodolphe Le Targat for the laser distribution.

REFERENCES

1. X. Yi, S. Hu, H. Zhou, C. Tang, B. Xu, J. Zhang, and K. Qiu, IEEE Photon. J. **8**, 1 (2016).
2. A. Belmonte, Opt. Lett. **40**, 1869 (2015).
3. J. Chen, Q. Liu, X. Fan, and Z. He, Opt. Lett. **41**, 1066 (2016).
4. J. L. Doménech and M. Cueto, Opt. Lett. **38**, 4074 (2013).
5. X. Xie, R. Bouchand, D. Nicolodi, M. Giunta, W. Hänsel, M. Lezius, A. Joshi, S. Datta, C. Alexandre, M. Lours, P. Tremblin, G. Santarelli, R. Holzwarth, and Y. L. Coq, Nat. Photonics **11**, 44 (2016).
6. R. L. Targat, L. Lorini, Y. L. Coq, M. Zawada, J. Guéna, M. Abgrall, M. Gurov, P. Rosenbusch, D. G. Rovera, B. Nagórny, R. Gartman, P. G. Westergaard, M. E. Tobar, M. Lours, G. Santarelli, A. Clairon, S. Bize, P. Laurent, P. Lemonde, and J. Lodewyck, Nat. Commun. **4**, 2109 (2013).
7. M. J. Thorpe, L. Rippe, T. M. Fortier, M. S. Kirchner, and T. Rosenband, Nat. Photonics **5**, 688 (2011).
8. S. Häfner, S. Falke, C. Grebing, S. Vogt, T. Legero, M. Merimaa, C. Lisdat, and U. Sterr, Opt. Lett. **40**, 2112 (2015).
9. L. Wu, Y. Jiang, C. Ma, W. Qi, H. Yu, Z. Bi, and L. Ma, Sci. Rep. **6**, 24969 (2016).
10. G. D. Cole, W. Zhang, B. J. Bjork, D. Follman, P. Heu, C. Deutsch, L. Sonderhouse, J. Robinson, C. Franz, A. Alexandrovski, M. Notcutt, O. H. Heckl, J. Ye, and M. Aspelmeyer, Optica **3**, 647 (2016).
11. O. Llopis, P. H. Merrer, H. Brahimi, K. Saleh, and P. Lacroix, Opt. Lett. **36**, 2713 (2011).
12. T. N. Huynh, L. Nguyen, and L. P. Barry, J. Lightwave Technol. **31**, 1300 (2013).
13. D. Xu, F. Yang, D. Chen, F. Wei, H. Cai, Z. Fang, and R. Qu, Opt. Express **23**, 22386 (2015).
14. A. J. Walsh, J. A. O'Dowd, V. M. Bessler, K. Shi, F. Smyth, J. M. Dailey, B. Kelleher, L. P. Barry, and A. D. Ellis, Opt. Lett. **37**, 1769 (2012).
15. S. Camatel and V. Ferrero, J. Lightwave Technol. **26**, 3048 (2008).
16. T. Okamoto and F. Ito, J. Lightwave Technol. **32**, 3119 (2014).
17. K. Kikuchi and K. Igarashi, in *Optical Fiber Communication Conference/National Fiber Optic Engineers Conference*, OSA Technical Digest (CD) (Optical Society of America, 2011), paper OML3.
18. E. Rubiola and V. Giordano, Rev. Sci. Instrum. **71**, 3085 (2000).
19. D. Eliyahu, D. Seidel, and L. Maleki, in *Proceedings of IEEE International Frequency Control Symposium (IFCS)* (2008), pp. 811–814.
20. C. Nelson and D. Howe, in *Proceedings of IEEE International Frequency Control Symposium (IFCS)* (2012), pp. 1–4.
21. D. Nicolodi, R. Bouchand, M. Lours, X. Xie, Y. L. Coq, M. Giunta, M. Lezius, W. Haensel, R. Holzwarth, P. Tremblin, G. Santarelli, S. Datta, A. Joshi, and C. Alexandre, in *Proceedings of IEEE International Frequency Control Symposium (IFCS)* (2016), pp. 1–3.
22. T. Liu, Y. N. Zhao, V. Elman, A. Stejskal, and L. J. Wang, Opt. Lett. **34**, 190 (2009).
23. A. Premoli and P. Tavella, IEEE Trans. Instrum. Meas. **42**, 7 (1993).
24. R. Drever, J. Hall, F. Kowalski, J. Hough, G. Ford, A. Munley, and H. Ward, Appl. Phys. B **31**, 97 (1983).
25. L. Ma, P. Jungner, J. Ye, and J. L. Hall, Opt. Lett. **19**, 1777 (1994).
26. J. Zhang, X. H. Shi, X. Y. Zeng, X. L. Lü, K. Deng, and Z. H. Lu, Rev. Sci. Instrum. **87**, 123105 (2016).
27. D. B. Sullivan, D. W. Allan, D. A. Howe, and F. L. Walls, NIST Technical Note 1337 (National Institute of Standards and Technology, 1990).
28. D. Nicolodi, B. Argence, W. Zhang, R. L. Targat, G. Santarelli, and Y. L. Coq, Nat. Photonics **8**, 219 (2014).